Quantifying Axonal Injury, Demylination, and inflammation in Human MS Autopsy Specimens using Diffusion Basis Spectrum Imaging (DBSI)

Yong Wang[1], Qing Wang[1], Mingqiang Xie[2], Anne H. Cross[2], and Sheng-Kwei Song[1]
[1]*Radiology, Washington University in St. Louis, Saint Louis, MO, United States,* [2]*Neurology, Washington University in St. Louis, Saint Louis, MO, United States*

Introduction:
To a first approximation, axon bundles have been considered as an aggregate of cylindrical tubes representing myelinated axon fibers. Such simplification has served the diffusion MRI community well in developing various techniques to resolve complications of crossing fibers and edema. In real life, typical axon bundles contain oligodendrocytes and other cells. During CNS pathology, cell components such as microglia and astrocytes may increase in numbers, and additional inflammatory cells, such as macrophages and lymphocytes, may enter from the blood. We contend that the presence of these cells significantly confounds white matter structure and pathology assessed using diffusion MRI. For example, the presence of a restricted diffusion component consisting of infiltrating cells will interfere with axonal fiber caliber estimation if not considered. The presence of infiltrating inflammatory cells will tend to reduce axial diffusivity leading to a false overestimation of axonal injury within white matter tracts. To address this issue, we have recently developed a new diffusion MRI method, diffusion basis spectrum imaging (DBSI) [1], demonstrating the capability to accurately quantify the extent of cellularity change as well as the axonal injury and demyelination in cuprizone treated mice. In the present study, autopsied spinal cord specimens of MS patients were examined to correlate DBSI with immunohistochemistry (IHC) findings.

Method:
Autopsy Spinal Cord Specimens: Ten autopsied human cervical spinal cords were fixed in 10% formalin and prepared for MRI scanning.
MRI: Diffusion MRI of the autopsy spinal cord specimens was performed using an Agilent DirectDrive console equipped with a 4.7 T magnet and a 15-cm inner diameter, actively shielded Magnex gradient coil (60 G/cm, 270 μs rise time). The tissue contained in a 3-ml syringe was placed in a custom-made solenoid coil for data acquisition using the following parameters: repetition time (TR) 2s, spin echo time (TE) 39 ms, time between application of gradient pulses (Δ) 20 ms, diffusion gradient duration (δ) 8 ms, slice thickness 0.5 mm, number of slices 5, field-of-view 2.4 × 2.4 cm^2, number of average 1, data matrix 192 × 192, SNR = 200. Diffusion sensitizing gradients were applied in 99 directions with max b-value = 3200 s/mm^2 [1]. In-plane resolution was 125 × 125 μm^2. Total acquisition time of diffusion weighted data was 5 hours and 20 minutes.
DBSI Analysis: The Eq. [1] was solved by fitting the 99 diffusion weighted signals using a linear combination of diffusion basis set consisting of cylindrically symmetric diffusion tensors [1] with the freedom to vary $\lambda_{||}$ and $\lambda_{\perp}$ to estimate the number of anisotropic diffusion tensor components (N_{aniso}) and the associated principal directions. After N_{Aniso} was computed, the number of

$$S_k = \sum_{i=1}^{N_{Aniso}} S_i e^{-\left|\vec{b}_k\right| \cdot \lambda_{\perp}} e^{-\left|\vec{b}_k\right| \cdot (\lambda_{||} - \lambda_{\perp}) \cos^2 \theta_i} + \sum_{j=1}^{N_{iso}} S_j e^{-\left|\vec{b}_k\right| \cdot d_j}, \qquad [1]$$

isotropic component (N_{iso}) was further determined using nonnegative least-squares (NNLS) analysis [2]. The global nonlinear optimization was conducted employing direct pattern search to solve Eq. [1]. A traditional derivative based optimization method was employed following the global optimization to improve the accuracy of the solution. The restricted isotropic components with mean ADC close to zero were assigned to cells [1].
Image Processing: DBSI/DTI maps were co-registered with IHC images using the previously published method [3] for both voxel-based and ROI analyses. An ROI analysis was employed after co-registration of MRI and IHC images. An investigator blinded to pathologic and clinical data independently identified regions of interest (ROI) from the T2W, DBSI, and DTI maps.

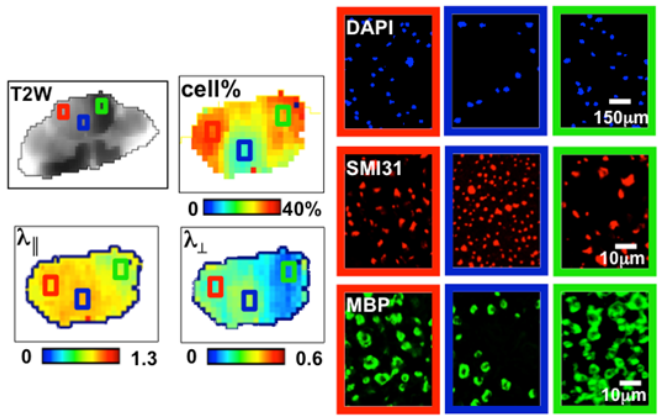

Figure 1. Ex vivo DBSI of a human MS autopsy spinal cord specimen. Regions of different pathology profiles are marked using red, blue, and green rectangles on T2W image. DBSI maps of cell %, $\lambda_{||}$, and $\lambda_{\perp}$ are presented in the expanded dorsal column and consistent with IHC findings. Red: increased cell infiltration with moderate axonal injury and demyelination; Blue: minor cell infiltration with severe demyelination and relatively preserved axon; Green: increased cell infiltration and axonal injury with relatively preserved myelin integrity.

Histology: After imaging, the formalin fixed MS spinal cord was embedded in paraffin and cut on a sliding microtome at a thickness of 5 μm. Paraffin sections were deparaffinized and rehydrated. Antigen was retrieved with 1 mM EDTA at 95 – 100°C water bath. All sections were blocked in 1% BSA for 1 h at room temperature to prevent nonspecific binding of antibodies and to increase permeability of antibodies. Sections were then incubated with monoclonal anti-myelin basic protein antidoby (MBP; 1:800; Abcam) and monoclonal anti-phosphorylated neurofilament H antibody (SMI-31; 1:2000; Sternberger Monoclonals) at 4°C overnight. After rinse, goat anti-mouse IgG conjugated with Alexa 488 (1:1500; Invitrogen) was applied to visualize immunoreactivity. After washing, sections were coverslipped in Vectashield Mounting Medium with 4',6'-diamidino-2-phenylindole (DAPI). Histological slides were examined with a Nikon Eclipse 80i fluorescence microscope equipped with a 20× objective, and images were captured with a black-white CCD camera using MetaMorph software.

Results and Discussion:
A representative cord was selected to demonstrate the capability of DBSI (Figure 1). Diffuse white matter injury was present in the dorsal column consistent with the recorded upper extremity numbness of the patient prior to death. Significantly increased cell infiltration was seen in all three ROIs comparing with the control (data not shown), green ≈ red (150% more than control) > blue (50% more than the control) in severity, consistent with DAPI staining. DBSI derived $\lambda_{||}$ at the red (0.81 ± 0.03 μm^2/ms) and the green (0.74 ± 0.03 μm^2/ms; total 16 voxels, p = 0.0005) ROIs are significantly different suggesting more axonal injury at the green ROI, consistent with the SMI-31 staining. In contrast, the effect of infiltrating cells on diffusion is evident by examining DTI derived $\lambda_{||}$ at the red (0.36 ± 0.02 μm^2/ms) and the green (0.31 ± 0.01 μm^2/ms; total 16 image voxels, p = 0.07) ROIs of the dorsal column. Compare to DBSI derived $\lambda_{||}$, DTI derived $\lambda_{||}$ are underestimated due to the increased cell infiltration at both red and green ROIs. In addition, DBSI derived $\lambda_{\perp}$ suggests that the severity of demyelination is blue > red > green, again consistent with the MBP staining. Current co-registered ROI analysis suggests that DBSI is consistent with IHC findings.

References: [1] Wang,Y. *et al*. *Brain*. 2011, In Press. [2] Lewis RM, *SIAM Journal on Optimization*. 1999;9(4):1082-99. [3] Budde, M. D. *et al. Magn Reson Med.* 2007; **57**: 688-695.